Inorganic Chemistry
Article

Inorg. Chem. **2010**, *49*, 9409–9415 **9409**
DOI: 10.1021/ic101200f

High Yield Precipitation of Crystalline α-Zirconium Phosphate from Oxalic Acid Solutions

Donatella Capitani,[†] Mario Casciola,[‡] Anna Donnadio,*[,‡] and Riccardo Vivani[‡]

[†]*Istituto di Metodologie Chimiche, Laboratorio di Risonanza Magnetica "Annalaura Segre", CNR, Via Salaria km 29.300, 00016 Monterotondo Scalo (RM), Italy, and* [‡]*Dipartimento di Chimica - CEMIN, via Elce di Sotto 8, 06123 Perugia, Italy*

Received June 18, 2010

Microcrystalline zirconium phosphate (ZrP) has been synthesized by precipitating a Zr(IV) salt (i.e., zirconium propionate, chloride, or oxide chloride) with H_3PO_4 from aqueous solutions of oxalic acid ($H_2C_2O_4$) at 80 °C. Independent of the Zr(IV) salt, crystalline materials have been obtained with reaction yields >90% and reaction time of one day for the following molar ratios: $H_3PO_4/Zr = 6$ and $H_2C_2O_4/Zr = 10$. The material prepared from Zr propionate (ZrP_{prop}) has been further investigated by scanning electron microscopy, thermogravimetry, and ion exchange titrations. Structural characterization has been performed by X-ray powder diffraction and solid state ^1H-^{31}P 2D correlation NMR experiments. Structural parameters obtained by Rietveld analysis of powder diffraction data agree with those reported in the literature for single crystal determinations. Moreover, NMR data show that the closest proton environment of the phosphorus atom in ZrP_{prop} is the same as in ZrP samples of similar crystallinity prepared according to literature methods.

1. Introduction

The chemistry of tetravalent transition metal phosphates has been known for over a century. In the past 40 years, these compounds have been the object of continuous interest in the chemical literature[1,2] because of their ion-exchange, intercalation, and ionic conduction properties. Among layered phosphates, monohydrate α-zirconium phosphate ($Zr(HPO_4)_2 \cdot H_2O$, hereafter ZrP) received a noticeable interest for its good thermal stability and excellent chemical inertia in strong acid media.[3]

In recent years, because of the possibility to obtain uniform dispersions of ZrP nanoparticles within polymeric matrixes, either by in situ growth or by exfoliation of preformed material, ZrP was used as a filler for the preparation of polymeric nanocomposites with improved physicochemical properties (e.g., reduced gas permeability, enhanced mechanical strength and thermal stability) in comparison with those of the pure polymer.[4−18]

Differently from in situ growth, the exfoliation of preformed ZrP microcrystals allows to control easily the aspect ratio of the particles of the exfoliated material through a suitable choice of the starting material since ZrP can be exfoliated without altering the size of the single layers:

*To whom correspondence should be addressed. E-mail: an.donnadio@libero.it. Phone: +39 075 5855568. Fax: +39 075 5855566.

(1) Alberti, G.; Casciola, M.; Costantino, U.; Vivani, R. *Adv. Mater.* **1996**, *8*, 291–303.
(2) Clearfield, A. *Solvent Extr. Ion Exch.* **2000**, *18*, 655–678. Trobajo, C.; Khainakov, S. A.; Espina, A.; García, J. R. *Chem. Mater.* **2000**, *12*, 1787–1790.
(3) Clearfield, A.; Costantino, U. Layered metal phosphates and their intercalation chemistry in Two and Three-Dimensional Inorganic Networks. In *Comprehensive Supramolecular Chemistry*; Alberti, G., Bein, T., Eds.; Pergamon, Elsevier Science ltd Press: New York, 1996; Vol. 7, Chapter 4.
(4) Alberti, G.; Casciola, M. In *Membrane Technology*; Peinemann, K. V., Nunes, S. P., Eds.; Wiley-VCH: Weinheim, 2008; Vol. 2, Chapter 4, pp 97−122.
(5) Casciola, M.; Capitani, D.; Comite, A.; Donnadio, A.; Frittella, V.; Pica, M.; Sganappa, M.; Varzi, A. *Fuel Cells* **2008**, *8*, 217–224.
(6) Casciola, M.; Bagnasco, G.; Donnadio, A.; Micoli, L.; Pica, M.; Sganappa, M.; Turco, M. *Fuel Cells* **2009**, *9*, 394–400.
(7) Hou, H.; Sun, G.; Wu, Z.; Jin, W.; Xin, Q. *Int. J. Hydrogen Energy* **2008**, *33*, 3402–3409.
(8) Chen, L. C.; Yu, T. L.; Lin, H. L.; Yeh, S. H. *J. Membr. Sci.* **2008**, *307*, 10–20.
(9) Arbizzani, C.; Donnadio, A.; Pica, M.; Sganappa, M.; Varzi, A.; Casciola, M.; Mastragostino, M. *J. Power Sources* **2010**, *195*, 7751–7756.
(10) Bongiovanni, R.; Casciola, M.; Di Gianni, A.; Donnadio, A.; Malucelli, G. *Eur. Polym. J.* **2009**, *45*, 2487–2493.
(11) Sue, H. J.; Gam, K. T.; Bestaoui, N.; Spurr, N.; Clearfield, A. *Chem. Mater.* **2004**, *16*, 242–249.
(12) Sun, L. Y.; Boo, W. J.; Browning, R. L.; Sue, H. J.; Clearfield, A. *Chem. Mater.* **2005**, *17*, 5606–5609.
(13) Liu, J.; Boo, W. J.; Clearfield, A.; Sue, H. J. *Mater. Manuf. Processes* **2006**, *20*, 143–151.
(14) Boo, W. J.; Sun, L. Y.; Liu, J.; Clearfield, A.; Sue, H. J.; Mullins, M. J.; Pham, H. *Compos. Sci. Technol.* **2007**, *67*, 262–269.
(15) Boo, W. J.; Sun, L.; Warren, G. L.; Moghbelli, E.; Pham, H.; Clearfield, A.; Sue, H. J. *Polymer* **2007**, *48*, 1075–1082.
(16) Sun, L.; Boo, W. J.; Sun, D.; Clearfield, A.; Sue, H. J. *Chem. Mater.* **2007**, *19*, 1749–1754.
(17) Sun, L.; Boo, W. J.; Sun, D.; Sue, H. J.; Clearfield, A. *New J. Chem.* **2007**, *31*, 39–43.
(18) Boo, W. J.; Sun, L.; Liu, J.; Clearfield, A.; Sue, H. J. *J. Phys. Chem. C* **2007**, *111*, 10377–10381.

Published on Web 09/20/2010

the exfoliation of large crystals leads therefore to the formation of high aspect ratio particles.[19]

The use of microcrystalline ZrP as a source of filler nanoparticles for polymer nanocomposites on a larger scale than the laboratory scale requires the availability of a quick and simple synthetic procedure, characterized by high yield and low environmental impact.

Early methods to prepare microcrystalline zirconium phosphate are based on rapid precipitation−reflux (I)[20] and on direct precipitation in the presence of hydrofluoric acid (II).[21] According to method (I) an amorphous ZrP gel, precipitated from $ZrOCl_2$ and H_3PO_4 solutions, is refluxed in H_3PO_4: the products obtained have different degrees of crystallinity and different particle sizes depending on the phosphoric acid concentration and on the refluxing time; truly crystalline ZrP is obtained after prolonged refluxing (up to 2 weeks) in 12 M H_3PO_4.

Method (II) consists in the decomposition of zirconium fluorocomplexes (usually at 80 °C) in the presence of phosphoric acid. A high yield precipitation takes some days and leads to the formation of highly crystalline material. To obtain yields as high as about 70%, the fluorocomplex decomposition is usually achieved by hydrofluoric acid evaporation at 80 °C, and this is the main environmental drawback of such a method.

Highly crystalline ZrP can also be prepared by hydrothermal synthesis at 170−200 °C (method (III)) starting from zirconium oxide chloride and phosphoric acid.[16,22] It was recently shown that, the reaction time being the same (i.e., 24 h), method (II) allows to obtain the larger microcrystals in comparison with methods (I) and (III).

Other synthetic approaches, including sol−gel methods based on the use of zirconium isopropoxide and different phosphate precursors,[23] lead to the formation of less crystalline ZrP samples than those prepared by method (II).

On the basis of the above considerations, we tried to modify method (II) so as to avoid the use of hydrofluoric acid and to obtain, at the same time, highly crystalline ZrP with high yield and shorter time than that required by the literature methods. This goal was reached by replacing hydrofluoric acid with oxalic acid. In the present paper, the structural features and some physicochemical properties of ZrP obtained with this procedure are compared with those of ZrP precipitated from HF solutions by means of X-ray powder diffraction, bidimensional solid state NMR, electron microscopy, thermogravimetric analysis, and ion-exchange reactions.

2. Experimental Section

2.1. Chemicals. Reagents were supplied by Magnesium Elektron Ltd., England (zirconyl propionate, $ZrO_{1.27}(C_2H_5COO)_{1.46}$ $1.6H_2O$, MW = 248 Da), Fluka (oxalic acid and 85% orthophosphoric acid), Merck (zirconium oxide chloride), Riedel-de-Haën (zirconium tetrachloride). All reagents were used as received without further purification.

2.2. Material Preparation. ZrP microcrystals were prepared according to three different synthetic procedures: (1) direct precipitation in the presence of oxalic acid (oxalic acid method), (2) direct precipitation in the presence of hydrofluoric acid (HF method), and (3) refluxing of amorphous ZrP in phosphoric acid (refluxing method).

2.2.1. Oxalic Acid Method. A weighed amount of a zirconium(IV) salt (i.e., zirconium propionate, zirconium tetrachloride or zirconium oxide chloride) was solubilized, under stirring at room temperature, in 35 mL of an aqueous solution of oxalic acid so that the Zr(IV) concentration was 0.1 M and the $H_2C_2O_4$/Zr molar ratio was in the range 4 to 10. Then a suitable volume of 14.8 M H_3PO_4 was added so that the H_3PO_4/Zr molar ratio was in the range 2 to 6. The resulting solution was heated for 24 h at 80 °C in a closed plastic bottle.

The precipitate thus obtained was separated from the solution by centrifugation at 3000 rpm, washed three times with 10^{-3} M HCl, dried overnight at 80 °C, and finally kept in a desiccator over a saturated $Mg(NO_3)_2 \cdot 6H_2O$ solution (53% relative humidity).

2.2.2. HF Method. Direct precipitation of crystalline ZrP from $ZrOCl_2$ and H_3PO_4 solutions, in the presence of hydrofluoric acid, was performed according to ref 21.

2.2.3. Refluxing Method. An aqueous solution of 0.5 M $ZrOCl_2 \cdot 8H_2O$ and 4 M HCl was added drop by drop to a solution of 2 M H_3PO_4 so that the H_3PO_4/Zr molar ratio was 11. The precipitate thus obtained was left at rest for 2 days, washed four times with 0.4 M H_3PO_4 (about 10 mL washing solution per gram of solid), three times with water and refluxed in 7 M H_3PO_4 for 60 h. The solid was then washed several times with 0.01 M HCl (until the H_3PO_4 concentration in the washing solution was lower than 3×10^{-4} M), and finally with deionized water. The solid was dried in air and stored at 53% relative humidity.

2.3. Techniques. Routine X-ray powder diffraction patterns were collected with a Panalytical X′Pert PRO diffractometer and a PW3050 goniometer equipped with an X′Celerator detector using the Cu−Kα radiation source with 2θ step size of 0.0170° and step scan of 20s. The LFF ceramic tube operated at 40 kV, 40 mA.

To minimize preferred orientations, the samples were carefully side-loaded onto a glass sample holder. The same amount of sample (0.1 g) was used in all experiments. About 10% in weight of lanthanum hexaboride, LaB_6, provided by The Gem Dugout, Deane K. Smith, 1652 Princeton Drive, State College, PA 16803 was added as an internal line standard to the zirconium phosphate samples used in the Rietveld refinements.

Rietveld refinements were performed with the GSAS program.[24] Unit cell parameters provided by The Gem Dugout were adopted for lanthanum boride (a = 4.1566 Å) and were not refined. Structural parameters of lanthanum boride were taken from ref 25 and were gently refined. Data coming from single crystal structure determination by Troup and Clearfield[26] were adopted as starting model for zirconium phosphate. Scale factors, background (14 terms shifted Chebyschev function), sample displacement, cell parameters for ZrP and peak profiles were first refined. Atomic parameters were then refined. All the atoms were refined isotropically, and neutral atomic scattering factors were used. Thermal displacement parameters of heavy atoms (Zr and P) were refined independently, while those of light oxygen atoms were refined by constraining the program to apply the same shifts. The shape of the profile was modeled by a pseudo-Voigt function (9 parameters) in which two parameters for asymmetry at low angle were included[27]

(19) Casciola, M.; Alberti, G.; Donnadio, A.; Pica, M.; Bottino, A.; Piaggio, P. *J. Mater. Chem.* **2005**, *15*, 4262–4267.
(20) Clearfield, A.; Stynes, J. A. *J. Inorg. Nucl. Chem.* **1964**, *26*, 117–129.
(21) Alberti, G.; Torracca, E. *J. Inorg. Nucl. Chem.* **1968**, *30*, 317–318. Alberti, G.; Allulli, S.; Costantino, U.; Massucci, M. A. *J. Inorg. Nucl. Chem.* **1975**, *37*, 1779–1786.
(22) Clearfield, A.; Smith, G. D. *Inorg. Chem.* **1969**, *8*, 431–436.
(23) Benhamza, H.; Barboux, P.; Bouhaouss, A.; Josien, F. A.; Livage, J. *J. Mater. Chem.* **1991**, *1*, 681–684. Ali, A. F.; Hanna, A. A.; Gad, A. E. *Phosphorus Res. Bull.* **2008**, *22*, 32–40.
(24) Larson, A.; Von Dreele, R. B. *GSAS, Generalized Structure Analysis System*; Los Alamos National Laboratory: Los Alamos, NM, 2001.
(25) Booth, C. H.; Sarrao, J. L.; Hundley, M. F.; Cornelius, A. L.; Kwei, G. H.; Bianchi, A.; Lawrence, J. M. *Phys. Rev. B* **2001**, *63*, 224302.
(26) Troup, J. M.; Clearfield, A. *Inorg. Chem.* **1977**, *16*, 3311–3314.
(27) Thompson, P.; Cox, D. E.; Hastings, J. B. *J. Appl. Crystallogr.* **1987**, *20*, 79–83. Finger, L. W.; Cox, D. E.; Jephcoat, A. P. *J. Appl. Crystallogr.* **1994**, *27*, 892–900.

A March-Dollase correction[28] along the *00l* direction was applied for preferred orientation; no stereochemical restraints were introduced, and no correction was applied for absorption. At the end of the refinement, the shifts in all parameters were less than their standard deviations.

Ion exchange titrations were performed with a Radiometer automatic titrimeter (TIM900 Titrilab and ABU91Buret); a sample of 0.1 g α-ZrP was suspended under stirring in 10 mL of 0.1 M NaCl and titrated by adding 0.1 mL of 0.1 M NaOH every 60 s.

Thermogravimetric determinations were carried out in an air flow by a NETZSCH STA 449 Jupiter thermal analyzer connected to a NETZSCH TASC 414/3 A controller at a heating rate of 10 °C min^{-1}.

The morphology of the powders was investigated with a Philips XL30 Scanning Electron Microscope (SEM). All samples were coated with a thin layer of gold before SEM observation.

ICP Varian Liberty ICP-OES with axial inject was used for the quantitative analysis of zirconium and phosphorus. The emission radiation was measured and amplified by a photomultiplication at 213.618 and 339.198 nm for phosphorus and zirconium, respectively. The determination of zirconium and phosphorus was carried out by calibration curve with standard solutions of phosphorus and zirconium. The samples to be analyzed were dried overnight in oven at 140 °C and weighed. The samples were then dissolved in a boiling solution of 1 M oxalic acid.

Solid state NMR experiments were performed on a Bruker Avance 400 spectrometer at resonance frequencies of 400.13 MHz for ^{1}H and 161.97 MHz for ^{31}P. Powdered samples were packed into 4 mm zirconia rotors and sealed with Kel-F caps. The spin-rate was 9794 Hz.

^{31}P CP-MAS spectra were performed with a contact time of 2 ms, the $\pi/2$ pulse width was 3.0 μs, the recycle delay was 3 s. Spectra were acquired using 1024 data points in the time domain, zero filled and Fourier transformed with a size of 2048 data points.

The heteronuclear ^{31}P-^{1}H correlation experiments were performed with the frequency-switched Lee−Goldburg homonuclear decoupling.[29] The duration of the successive FS-LG pulses was optimized to 10.2 μs, the magic angle pulse length was 2.13 μs; 64 slices were collected in the f1 dimension, and the number of scans was 32. A short contact time, 100 μs, was purposely used to obtain correlation only between phosphorus and neighbor protons.

^{1}H and ^{13}P chemical shifts were referenced to glucose 6-phosphate which was added as an internal reference. Glucose 6-phosphate was previously solubilized in D_2O and frozen dried to convert all exchangeable OH groups to OD groups. The phosphorus resonance of glucose 6-phosphate was set at 3.8 ppm from an 1 M H_3PO_4/D_2O solution, and methylene protons of glucose 6-phosphate were set to 4 ppm from TMS.

3. Results and Discussion

In a first series of experiments, crystalline ZrP samples (ZrP_{ox}) were precipitated at 80 °C in the presence of oxalic acid from solutions of phosphoric acid and different zirconium salts (zirconium tetrachloride, zirconium oxide chloride, and zirconium propionate) with H_3PO_4/Zr molar ratios in the range 2 to 6 and $H_2C_2O_4/Zr = 10$. In all cases, a white non-gelatinuos precipitate began settling just after heating had started. X-ray powder patterns of the wet precipitate, collected at regular time intervals during 1 day, showed that the intensity and the width of the diffraction peaks did not change significantly after about 15 h of heating. Nevertheless, all data reported in the following refer to materials obtained with 24 h of heating at 80 °C.

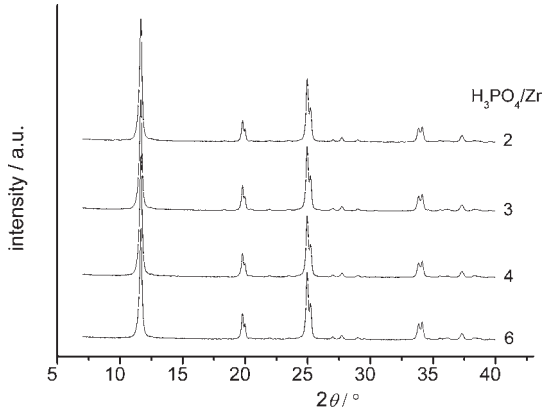

Figure 1. X-ray powder patterns of ZrP_{ox} samples precipitated from zirconium propionate solutions with $H_2C_2O_4/Zr = 10$ and the indicated H_3PO_4/Zr molar ratios.

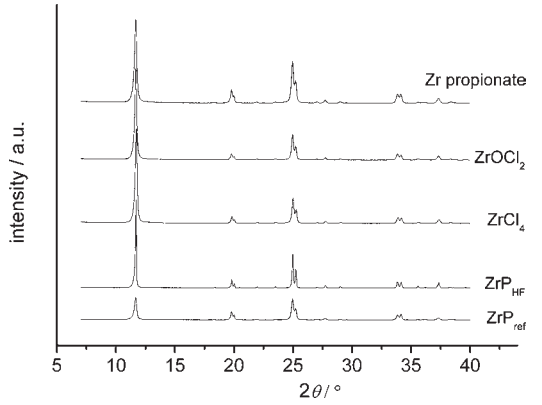

Figure 2. X-ray powder patterns of ZrP_{ox} samples precipitated from solutions of the indicated zirconium salts with $H_2C_2O_4/Zr = 10$ and $H_3PO_4/Zr = 6$. The patterns of ZrP_{HF} and ZrP_{ref} sanples are reported for comparison.

Representative X-ray powder patterns are shown in Figures 1 and 2 and compared with the patterns of two ZrP samples prepared according to the HF method (ZrP_{HF}) and the refluxing method (ZrP_{ref}). While all patterns show the same reflections, the intensity of the reflections of ZrP_{ox} samples is nearly independent of the H_3PO_4/Zr molar ratio and of the nature of the zirconium salt thus indicating that, within the investigated range, the composition of the mother solution does not affect the precipitate crystallinity. Comparison of ZrP_{ox} patterns with those of ZrP_{HF} and ZrP_{ref} shows that the ZrP_{ox} reflections are as intense as those of ZrP_{HF} and more intense than those of ZrP_{ref}. Therefore, direct precipitation in the presence of oxalic acid allows the formation of crystalline ZrP in much shorter time (1 day) than that (several days) required for the procedures based on refluxing in phosphoric acid and on direct precipitation in the presence of HF.

The reaction yield is nearly independent of the nature of the zirconium salt but is strongly affected by the H_3PO_4/Zr ratio and increases from ≈45% to ≈95% when the H_3PO_4/Zr ratio increases from 2 to 6 (Figure 3).

In a second series of experiments, ZrP samples were precipitated from zirconium propionate solutions with $H_3PO_4/Zr = 6$ and $H_2C_2O_4/Zr$ ranging from 4 to 10. The X-ray

(28) Dollase, W. A. *J. Appl. Crystallogr.* **1986**, *19*, 267.
(29) Van Rossum, B. J.; Förster, H.; De Groot, H. J. M. *J. Magn. Reson.* **1997**, *124*, 516–519.

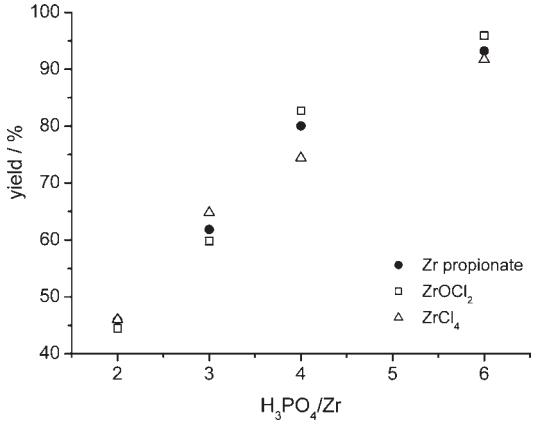

Figure 3. Reaction yield for the precipitation of ZrP_{ox} samples from solutions of the indicated zirconium salts with $H_2C_2O_4/Zr = 10$.

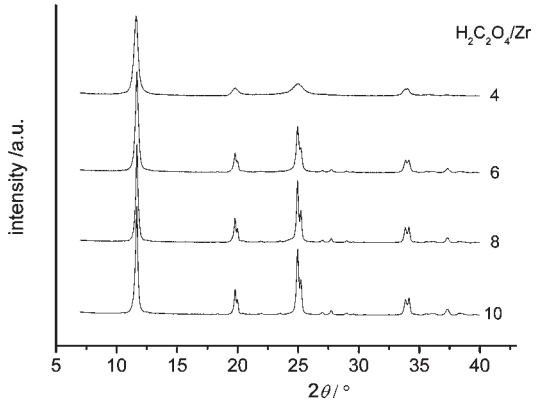

Figure 4. X-ray powder patterns of ZrP_{ox} samples precipitated from zirconium propionate solutions with $H_3PO_4/Zr = 6$ and the indicated $H_2C_2O_4/Zr$ molar ratios.

powder patterns of these samples (Figure 4) are characterized by an increase in the peak intensity and a decrease in the peak width with increasing the $H_2C_2O_4/Zr$ ratio, especially from 4 to 6. Correspondingly, the reaction yield goes from 58% to 86% (Figure 5) mainly because of the reduced peptization the precipitate undergoes during washing.

On the basis of the above findings, ZrP_{ox} samples precipitated from zirconium propionate solutions with molar ratios $H_2C_2O_4/Zr = 10$ and $H_3PO_4/Zr = 6$ were chosen for further characterization work.

3.1. SEM Images. SEM microphotographs of ZrP_{ox}, ZrP_{HF}, and ZrP_{ref} samples are shown in Figure 6. It is apparent that ZrP_{ox} consists of aggregates of thin platelets with an average size of 2−3 μm, while ZrP_{HF} microcrystals show a larger size distribution mainly in the range from 5 to 10 μm. On the contrary, ZrP_{ref} is formed by very small and rather homogeneous crystals with a size of 100−200 nm. Although the pictures of Figure 6 do not allow an accurate estimation of the particle thickness, it is evident that the particle aspect ratio decreases in the order $ZrP_{ox} > ZrP_{HF} > ZrP_{ref}$.

3.2. Thermal Analysis. Weight loss curves of ZrP_{ox}, ZrP_{HF}, and ZrP_{ref} are shown in Figure 7. All samples lose two water molecules per unit formula because of the loss of crystallization water and to the subsequent ≡POH condensation leading to the formation of layered ZrP_2O_7, which converts into cubic ZrP_2O_7 above about 900 °C.

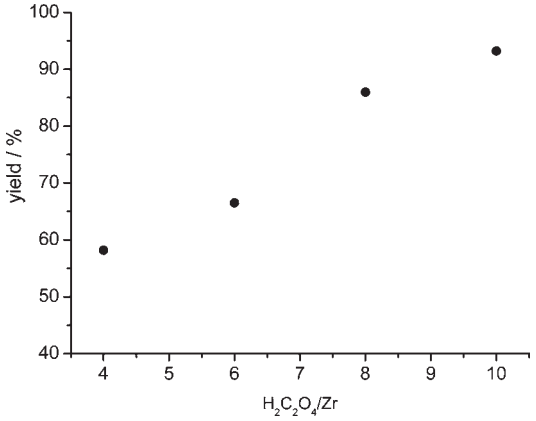

Figure 5. Reaction yield for the precipitation of ZrP_{ox} samples from zirconium propionate solutions with $H_3PO_4/Zr = 6$ as a function of $H_2C_2O_4/Zr$ molar ratio.

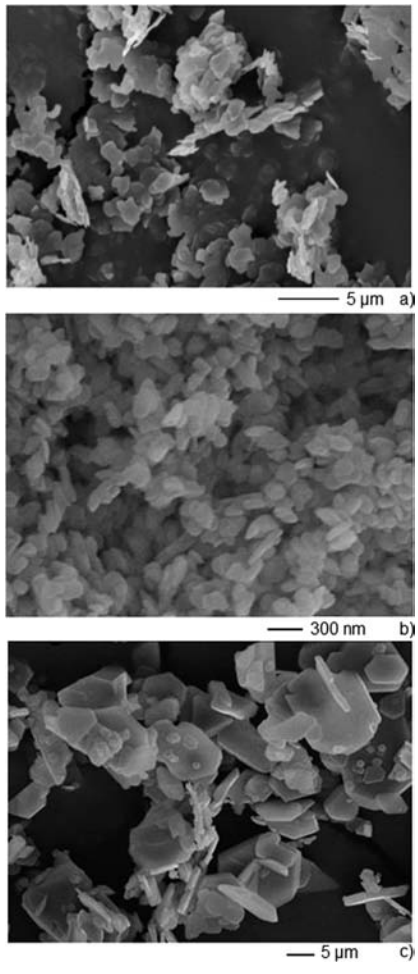

Figure 6. SEM pictures of ZrP_{ox} (a), ZrP_{ref} (b), and ZrP_{HF} (c) samples.

However, the different crystal size is associated with fairly distinct thermal behaviors: with increasing crystal size, the loss of crystallization water is progressively shifted toward high temperature and hence less separated from the loss of condensation water.

In particular, ZrP_{ref} loses the first water molecule between 70 and 150 °C and the second one between 400 and 650 °C. ZrP_{HF} loses only about 0.4 water molecules between 70 and 200 °C, while the loss of the remaining 0.6

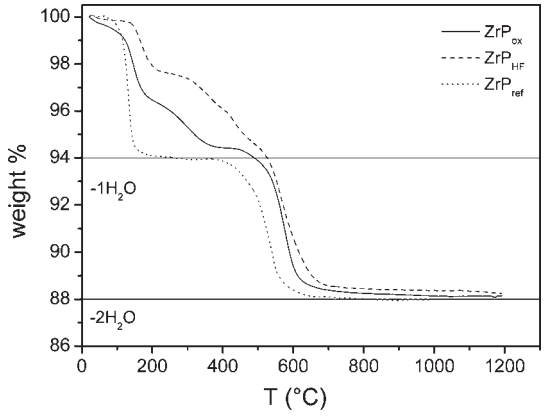

Figure 7. Weight loss curves of ZrP_{ox}, ZrP_{HF}, and ZrP_{ref} samples.

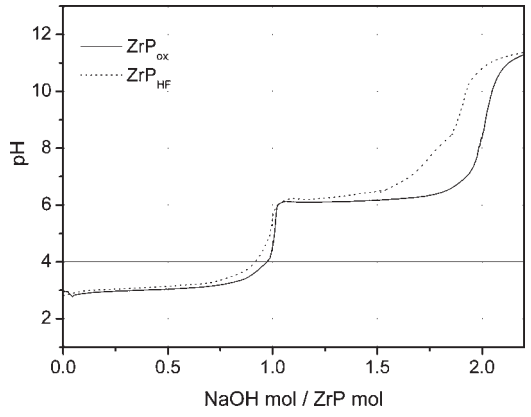

Figure 8. Titration curves of ZrP_{ox} and ZrP_{HF} samples.

crystallization water molecules occurs in the range 260−530 °C just before the loss of condensation water. The thermogravimetric curve of ZrP_{ox} is intermediate between those of ZrP_{ref} and ZrP_{HF}, with a short plateau between 380 and 450 °C separating the loss of crystallization water from the loss of condensation water.

3.3. Ion Exchange Properties. The ion exchange properties of ZrP_{ox} were investigated by titrating ZrP_{ox} microcrystals with 0.1 M NaOH (Figure 8). For comparison, ZrP_{HF} was titrated under the same experimental conditions. Titration curves for ZrP made by the reflux method in time periods of 24 h to greater than 336 h are provided by Clearfield et al.[30] along with the change in unit cell dimensions in space groups $P21/c$.

The titration curve of ZrP_{ox} shows two inflection points separated by two well-defined plateaux that are associated with the coexistence of couples of crystalline phases: $Zr(HPO_4)_2 \cdot H_2O$-$ZrHNa(PO_4)_2 \cdot 5H_2O$ (first plateau) and $ZrHNa(PO_4)_2 \cdot 5H_2O$-$Zr(NaPO_4)_2 \cdot 3H_2O$-(second plateau).[3] As expected, the second inflection point corresponds to the exchange of two sodium ions per ZrP unit formula.

The titration curves of ZrP_{ox} and ZrP_{HF} are nearly coincident in the first plateau, but differ significantly in the second half of the second plateau where, for the same pH value, ZrP_{HF} exchanges less sodium ion than ZrP_{ox}. Taking into account that the titration curves were collected with fixed time intervals between consecutive NaOH additions, the lower sodium uptake of ZrP_{HF} must be ascribed to a slower ion exchange kinetics because of the larger size of the ZrP_{HF} microcrystals. This is actually what is expected for ion exchange reactions occurring according to the so-called "moving phase boundary" mechanism[31] as is the case of Na^+/H^+ exchange in ZrP.

Table 1. Crystal Data and Refinement Details for ZrP_{ox} and ZrP_{HF}

	sample	
	ZrP_{ox}	ZrP_{HF}
empirical formula	$ZrP_2O_9H_4$	
formula weight	301.2	
crystal system	monoclinic	
space group	$P2_1/n$	
Z	4	
T/°C	25	
calculated density/g.cm^{-3}	2.76	
pattern range, 2θ/deg	4−140	
step scan increment, 2θ/deg	0.017	
step scan time/s	60	
R_p [a]	0.038	0.039
R_{wp} [b]	0.052	0.059
R_F2 [c]	0.078	0.072
χ [d]	2.61	3.27

[a] $R_p = \sum|I_o - I_c|/\sum I_o$. [b] $R_{wp} = [\sum w(I_o - I_c)^2/\sum wI_o^2]^{1/2}$. [c] $R_F2 = \sum|F_o^2 - F_c^2|/\sum|F_o^2|$. [d] $\chi = [\sum w(I_o - I_c)^2/(N_o - N_{var.})]^{1/2}$.

Table 2. Unit Cell Parameters for ZrP_{ox}, ZrP_{HF} and ZrP Single Crystals[26]

	a (Å)	b (Å)	c (Å)	β (deg)	V (Å^3)
ZrPox	9.0631(2)	5.2886(1)	15.4444(3)	101.717(2)	724.84(3)
ZrP_{HF}	9.0599(1)	5.28813(5)	15.4525(2)	101.697(1)	724.95(1)
s.c.	9.060(2)	5.297(1)	15.414(3)	101.71(2)	724.3(5)

3.4. Structural Features. Rietveld refinements were performed on ZrP_{ox} and ZrP_{HF} samples. Crystal data and details of the refinements are reported in Table 1, while Table 2 shows the refined unit cell parameters compared with those reported for single crystal determination.[26] Tables 3, 4, and 5 show atomic parameters, bond distances, and angles, respectively, for the three samples. Figure 9 shows the final Rietveld and difference plot for ZrP_{ox} and ZrP_{HF}.

The comparison of unit cell parameters for ZrP_{ox} and ZrP_{HF} reported in Table 2 shows a generally good agreement with the single crystal parameters. The main differences are found in the c axis, that is about 0.2% larger in the powder samples than in single crystal. This difference leads to a slight difference in the interlayer distance, calculated as $d = 0.5c \sin\beta$, which results to be 7.55 Å for single crystals and 7.56 Å for powder samples. Since the sheets are packed along the c axis with only weak van der Waals interactions,[32] this small difference may be originated by a lower (i.e., more negative) reticular energy associated with larger crystals.

ZrO_6 octahedra and PO_4 tetrahedra are more regular in the single crystal than in the powder samples; however, average Zr−O and P−O distances (Zr−O: 2.03 Å for ZrP_{ox}, 2.08 Å for ZrP_{HF} and 2.065 Å for s.c.; P−O: 1.55 Å

(30) Clearfield, A.; Kullberg, L.; Oskarsson, A. *J. Phys. Chem.* **1974**, *78*, 1150–1153.

(31) Alberti, G. Layered metal phosphates and their intercalation chemistry in Two and Three-Dimensional Inorganic Networks. In *Comprehensive Supramolecular Chemistry*; Alberti, G., Bein, T., Eds.; Pergamon, Elsevier Science ltd Press: New York, 1996; Vol. *7*, Chapter 1.

(32) Albertsson, J.; Oskarsson, A.; Tellgren, R.; Thomas, J. O. *J. Phys. Chem.* **1977**, *81*, 1574–1578.

Table 3. Fractional Atomic Coordinates for ZrP_{ox}, ZrP_{HF}, and ZrP Single Crystals[26]

name		*x*/*a*	*y*/*b*	*z*/*c*
Zr	ZrP_{ox}	0.2457(3)	0.251(2)	0.4855(1)
	ZrP_{HF}	0.2464(3)	0.250(2)	0.4860(1)
	s.c.	0.24609(2)	0.25261(5)	0.48506(2)
P2	ZrP_{ox}	0.3894(9)	0.757(4)	0.3894(4)
	ZrP_{HF}	0.3864(8)	0.745(4)	0.3862(4)
	s.c.	0.38744(7)	0.7508(1)	0.38567(4)
P3	ZrP_{ox}	−0.1327(8)	0.250(4)	0.3993(4)
	ZrP_{HF}	−0.1309(8)	0.245(4)	0.3978(4)
	s.c.	−0.13422(7)	0.2420(1)	0.39658(4)
O4	ZrP_{ox}	0.547(2)	0.797(4)	0.4398(8)
	ZrP_{HF}	0.542(2)	0.812(3)	0.4353(9)
	s.c.	0.5445(2)	0.8037(4)	0.4374(2)
O5	ZrP_{ox}	0.349(2)	0.481(4)	0.414(1)
	ZrP_{HF}	0.336(2)	0.497(4)	0.398(1)
	s.c.	0.3353(2)	0.4862(4)	0.4007(1)
O6	ZrP_{ox}	0.263(2)	0.968(4)	0.397(1)
	ZrP_{HF}	0.274(2)	0.954(4)	0.403(1)
	s.c.	0.2772(2)	0.9480(4)	0.4065(1)
O7	ZrP_{ox}	0.390(1)	0.775(5)	0.2860(6)
	ZrP_{HF}	0.388(1)	0.723(5)	0.2837(7)
	s.c.	0.3885(3)	0.7559(5)	0.2843(1)
O8	ZrP_{ox}	−0.199(2)	0.431(3)	0.451(1)
	ZrP_{HF}	−0.212(2)	0.429(3)	0.448(1)
	s.c.	−0.2180(2)	0.4364(4)	0.4404(2)
O9	ZrP_{ox}	−0.158(2)	−0.026(4)	0.428(1)
	ZrP_{HF}	−0.154(2)	−0.011(4)	0.432(1)
	s.c.	−0.1554(2)	−0.0205(4)	0.4316(1)
O10	ZrP_{ox}	−0.199(1)	0.248(7)	0.3011(6)
	ZrP_{HF}	−0.198(1)	0.267(6)	0.2979(7)
	s.c.	−0.1942(2)	0.2493(5)	0.2949(1)
O11	ZrP_{ox}	0.038(2)	0.332(3)	0.4163(8)
	ZrP_{HF}	0.033(2)	0.309(4)	0.4101(8)
	s.c.	0.0320(2)	0.3070(4)	0.4086(2)
O12	ZrP_{ox}	0.002(2)	0.727(4)	0.2613(7)
	ZrP_{HF}	−0.006(2)	0.719(3)	0.2621(8)
	s.c.	0.0042(3)	0.7241(5)	0.2617(2)

Table 4. Bond Distances for ZrP_{ox}, ZrP_{HF}, and ZrP Single Crystals[26]

	distance (Å)		
bond	ZrP_{ox}	ZrP_{HF}	s.c.
Zr−O4	2.01(1)	2.08(2)	2.048(2)
Zr−O5	2.00(2)	2.16(2)	2.074(2)
Zr−O6	2.06(2)	2.07(2)	2.071(2)
Zr−O8	2.03(2)	2.04(2)	2.054(2)
Zr−O9	2.07(2)	2.08(2)	2.065(2)
Zr−O11	2.02(2)	2.07(1)	2.075(2)
P2−O4	1.50(2)	1.50(2)	1.510(2)
P2−O5	1.57(3)	1.41(2)	1.512(2)
P2−O6	1.62(2)	1.56(2)	1.524(2)
P2−O7	1.60(1)	1.59(1)	1.564(2)
P3−O8	1.45(2)	1.52(2)	1.517(2)
P3−O9	1.56(3)	1.49(2)	1.518(2)
P3−O10	1.51(1)	1.54(1)	1.551(2)
P3−O11	1.57(2)	1.50(2)	1.519(2)
O12···O7	2.74(3)	2.97(3)	2.807(3)
O12···O10	2.72(2)	2.67(2)	2.769(3)

for ZrP_{ox}, 1.51 Å for ZrP_{HF} and 1.527 Å for s.c.) are similar in the three samples and are not systematically larger in powder than in a single crystal. For this, the slightly larger unit cell volume shown by both powder samples can be mainly associated to the extraframework domain, that is, to the packing of layers, while the layer frameworks are close to each other.

3.4. NMR Investigation. While X-ray diffraction does not allow to locate H atoms, solid state NMR can provide information on the local environment of H atoms, even in

Table 5. Bond Angles for ZrP_{ox}, ZrP_{HF}, and ZrP Single Crystals[26]

	amplitude (deg)		
angle	ZrP_{ox}	ZrP_{HF}	s.c.
O4−Zr−O5	84.6(8)	92.5(7)	91.14(8)
O4−Zr−O6	95.8(8)	91.6(7)	90.45(7)
O4−Zr−O8	95.1(9)	93.1(8)	89.76(8)
O4−Zr−O9	89.6(8)	89.1(7)	89.35(8)
O4−Zr−O11	174.5(11)	178.6(8)	178.85(8)
O5−Zr−O6	88.3(6)	87.6(6)	88.96(7)
O5−Zr−O8	86.0(9)	85.8(8)	88.88(7)
O5−Zr−O9	173.2(8)	178.3(8)	179.51(7)
O5−Zr−O11	94.2(7)	88.8(7)	89.96(7)
O6−Zr−O8	167.1(8)	172.0(8)	177.83(8)
O6−Zr−O9	95.8(9)	91.8(8)	91.04(7)
O6−Zr−O11	89.5(7)	88.9(8)	89.91(7)
O8−Zr−O9	91.0(8)	94.7(7)	91.12(7)
O8−Zr−O11	79.4(8)	86.5(7)	89.92(8)
O9−Zr−O11	91.3(7)	89.6(7)	89.55(7)
O4−P2−O5	104.3(15)	116.6(14)	112.4(1)
O4−P2−O6	118.7(16)	108.8(14)	110.5(1)
O4−P2−O7	108.2(9)	108.8(9)	109.2(1)
O5−P2−O6	114.7(12)	113.5(11)	111.4(1)
O5−P2−O7	110.2(16)	97.4(16)	103.6(1)
O6−P2−O7	100.5(13)	111.0(13)	109.6(1)
O8−P3−O9	111.3(13)	106.3(12)	110.6(1)
O8−P3−O10	115.5(17)	109.1(14)	109.2(1)
O8−P3−O11	103.1(15)	111.2(15)	111.4(1)
O9−P3−O10	103.2(19)	111.8(16)	109.8(1)
O9−P3−O11	113.9(14)	111.8(13)	111.0(1)
O10−P3−O11	110.2(9)	106.8(8)	104.7(1)
Zr−O4−P2	164.3(19)	156.7(14)	160.6(1)
Zr−O5−P2	149.2(13)	144.6(12)	145.5(1)
Zr−O6−P2	134.5(11)	143.7(12)	146.1(1)
Zr−O8−P3	163.9(15)	157.6(14)	157.5(1)
Zr−O9−P3	145.4(13)	151.2(13)	149.4(1)
Zr−O11−P3	144.2(12)	145.6(11)	145.8(1)

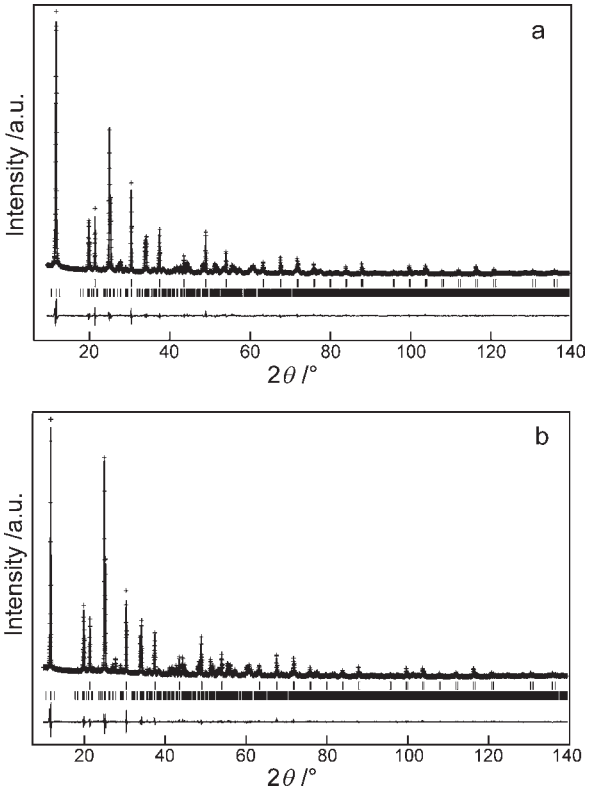

Figure 9. Final Rietveld and difference plot for ZrP_{ox} (a), and ZrP_{HF} (b). Marks indicate the calculated positions of LaB_6 (upper) and ZrP (lower) peaks.

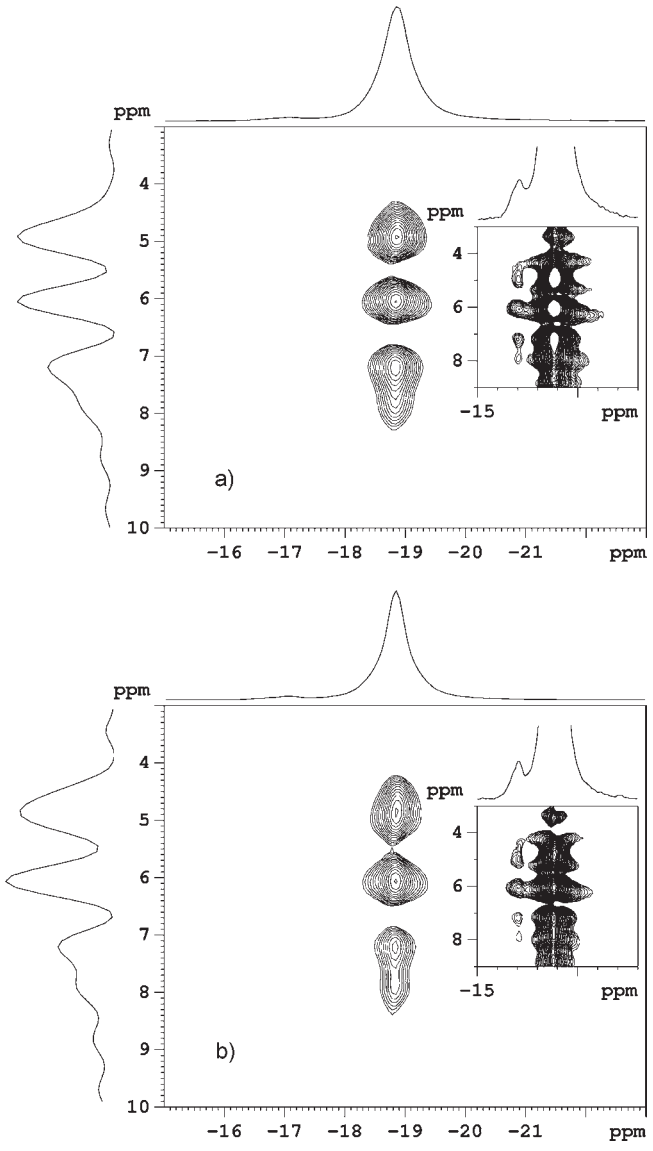

Figure 10. 2D solid state ^{1}H-^{31}P correlation spectra of sample ZrP_{ox} (a) and sample ZrP_{HF} (b). ^{31}P CP-MAS spectra are shown as projection in the f2 dimension, whereas ^{1}H spectra are shown as projection in the f1 dimension. The ^{1}H-^{31}P correlation spectra with a vertical multiplication of 2^4 are reported in the insets.

an amorphous environment. Therefore, to further compare the structural features of ZrP_{ox} and ZrP_{HF}, their ^{1}H-^{31}P correlation spectra were collected. These spectra are shown in Figure 10 together with the ^{31}P CP-MAS spectra reported as projections in the f2 dimension, whereas the ^{1}H spectra were obtained as projections and reported in the f1 dimension. In both correlation spectra the intense phosphorus resonance at −18.87 ppm, typical of the monohydrogen phosphate group bonded to three Zr(IV) atoms of the α-layer,[33] shows correlations with H atoms at 4.90, 6.07, 7.22 and, possibly, at 7.80 ppm. The resonances at 4.90 and 6.07 ppm are assigned to the H atoms of the water molecule since they disappear when ZrP is dehydrated.[18] Consequently the resonances at 7.22 and 7.80 ppm are associated with the acidic H atoms of the monohydrogen phosphate groups.

The ^{1}H-^{31}P correlation spectra with a vertical multiplication of 2^4 are reported in the insets of Figure 10. It is possible to observe that the very weak resonance at −17 ppm also shows correlations with protons at 4.90, 6.07, 7.22, and, possibly, at 7.80 ppm.

It is worth noting that the ^{1}H spectra reported in the f1 dimension of the 2D map of Figures 10a and 10b are very similar to each other, pointing out that also the closest proton environment of the phosphorus atom is the same in both investigated samples.

4. Conclusion

The procedure here reported for the synthesis of crystalline ZrP is a variant of the direct precipitation method proposed by Alberti where hydrofluoric acid is replaced by oxalic acid.

In comparison with the material prepared by the HF method, ZrP_{ox} has the same structural features, as inferred from X-ray and NMR data, and similar ion exchange and thermal behavior; on the other hand, ZrP precipitation from oxalic acid solutions has the advantage of achieving higher reaction yields and avoiding, at the same time, hydrofluoric acid evaporation. Moreover, the new procedure allows preparing fairly large ZrP microcrystals in much shorter time than the HF and refluxing methods do, and could be useful for large scale production of crystalline ZrP to be used as a filler of polymeric nanocomposites.

Finally, the oxalic acid method is expected to be suitable not only for the preparation of other insoluble phosphates of tetravalent metals but also for the synthesis of a large variety of zirconium phosphonates, as proven by preliminary experiments carried out in our laboratory.

Acknowledgment. This work was supported by Italian Ministry of University and Research (MIUR) under PRIN 2007 Project. The authors wish to thank Camilla Chianella, Federico Medori, and Manolo Sganappa for their contribution to the synthetic work.

(33) Clayden, N. J. *J. Chem. Soc., Dalton Trans.* **1987**, 1877–1881.